IOP Conference Series:
Materials Science and
Engineering

PURPOSE-LED PUBLISHING™

PAPER • **OPEN ACCESS**

Investigating the Effect of Laser Power and Scanning Strategy on Porosity in PBF-LB of 316L Stainless Steel

To cite this article: Mojtaba Miri Beidokhti *et al* 2025 *IOP Conf. Ser.: Mater. Sci. Eng.* **1332** 012021

View the article online for updates and enhancements.

You may also like

- Effect of laser power on microstructure and properties of Ti-Al/WC composite coatings
Hongwei Liu, Baoquan Dong, Xun Gong et al.
- Deformation and Fracture Behaviors in Microscale Laser Dynamic Flexible Forming: The Case of Fabricating Micro-Channel on Copper Foil
Songling Chen and Zongbao Shen
- Effect of laser power on the organization and properties of CoCrMo/TiC composite coatings
Huanming Sun, Di Wang, Hui Zhao et al.

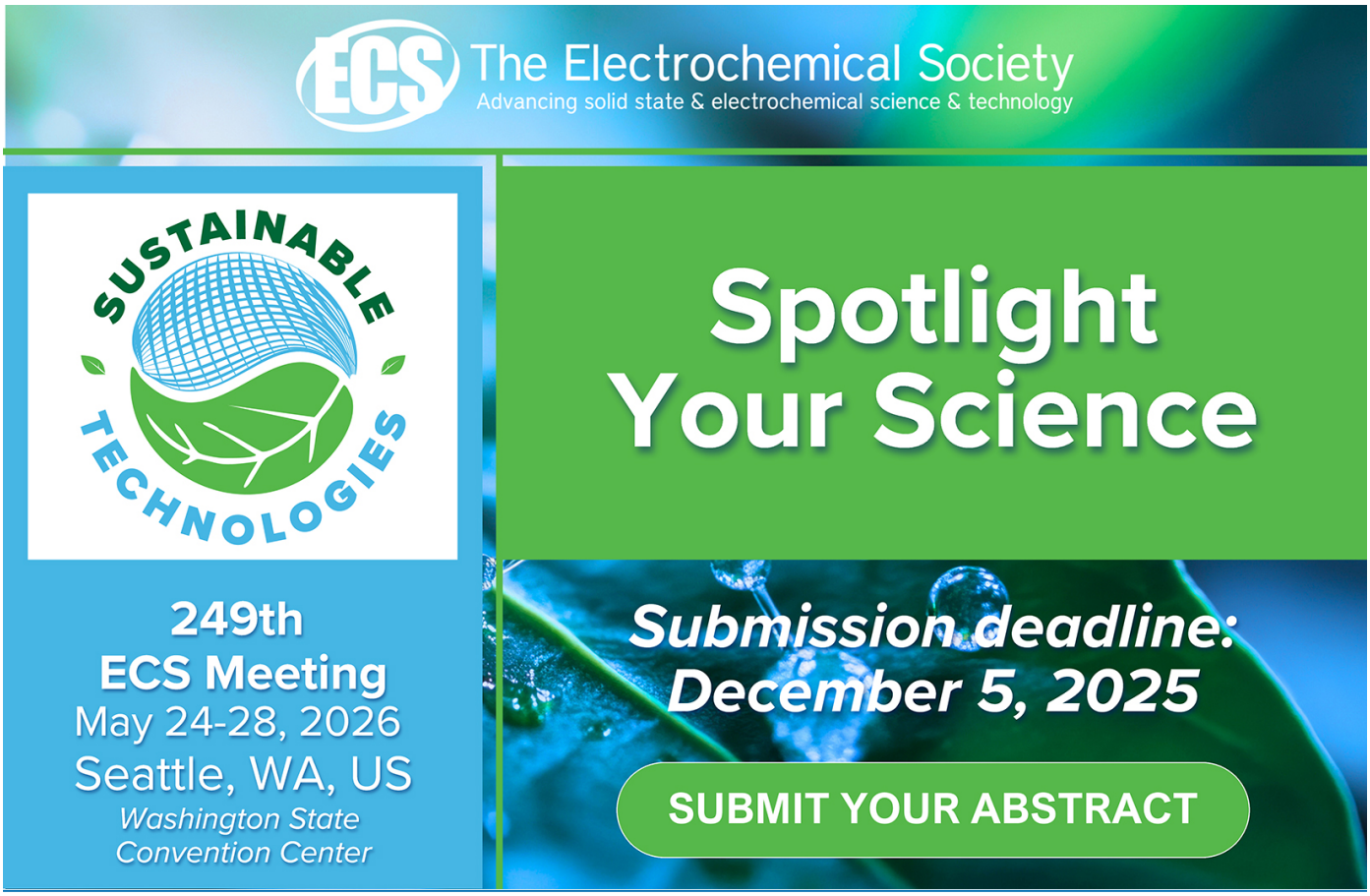

This content was downloaded from IP address 130.232.200.91 on 20/11/2025 at 11:50

IOP Conf. Series: Materials Science and Engineering **1332** (2025) 012021 doi:10.1088/1757-899X/1332/1/012021

Investigating the Effect of Laser Power and Scanning Strategy on Porosity in PBF-LB of 316L Stainless Steel

Mojtaba Miri Beidokhti[1*], Einari Tolvanen[1], Anum Rasheed[1] and Heidi Piili[1]

[1] Research Group of Digital Manufacturing and Surface Engineering (DMS), Department of Mechanical Engineering, Faculty of Technology, University of Turku, Turku, Finland

[*]E-mail: mmibei@utu.fi

Abstract. This study aims to investigate the influence of laser power and scanning strategy on the formation of macro-scale pores in laser-based powder bed fusion of metals (PBF-LB/M) for the manufacturing of 316L stainless steel. Samples were fabricated with varying laser powers and scanning strategies, and their porosity levels were analysed using optical microscopy and image analysis techniques. Volumetric energy density (VED) has been widely employed in previous studies as a comparative tool for integrating process parameters; however, its simplifications can obscure the influence of individual factors. In this study, laser power was found to have a significant effect on porosity formation, with an optimal *VED* value of 93 J/mm^3 minimizing defects. However, the impact of scanning strategy on porosity was inconclusive due to limited data. Future studies should focus on expanding the dataset to further assess scanning strategies and explore advanced methods to mitigate porosity-related defects, aiming to improve the reliability and performance of additively manufactured components.

1. Introduction

Additive manufacturing (AM) of metallic components is emerging as a transformative alternative to conventional production routes. Among AM techniques, laser-based powder bed fusion of metals (PBF-LB/M) is frequently highlighted for its ability to fabricate fully dense parts with complex geometries [12]. More than one hundred process parameters can be tuned; the most optimised are laser power, layer thickness, laser scan velocity, hatch spacing and scanning strategy [13]. Parameter changes have been shown to exert pronounced effects on porosity, surface texture and melt pool dimensions [6]. Porosity is one of the most common defects in parts manufactured via PBF-LB-M, other defects being, for example, distortion, delamination, balling, and stair-case e effect[11] Porosity can be defined as a void in the volume where there should be material. Voids can be considered as macro scale defects, and they can be relatively easily observed, for example, with optical microscopy [4]. A set of processing parameters that directly affect the relative density of the manufactured pieces govern the PBF-LB/M process. As a result, some research has been done to examine how processing parameters affect the emergence of defects in different structures [15, 16] The scan speed v (mm/s), laser power P (W), hatch distance h (mm), and powder bed thickness t (mm), in addition to a variety of other input process parameters, primarily control the process phenomena and, as a result, the overall qualities of the product. Volumetric energy density *VED* (J/mm^3) can be calculated as Equation 1 shows [7]

$$\boldsymbol{VED = \frac{P}{v*h*t}} \qquad (1)$$

Content from this work may be used under the terms of the Creative Commons Attribution 4.0 licence. Any further distribution of this work must maintain attribution to the author(s) and the title of the work, journal citation and DOI.
Published under licence by IOP Publishing Ltd

Many studies have tried to find optimum value for *VED* for different materials by varying these four parameters [5, 9] On the other hand, Ghorbanpour et al. [2] shows that even with the same *VED* the number of defects in the process can be vary depend on the combination of these four parameters. Scanning strategy refers to the path followed by the laser beam as it melts and fuses the metal powder. The choice of scanning strategy can influence the quality, mechanical properties, and defect formation like residual stress, porosity, microstructure, and grain orientation of the Additively Manufactured (AMed) parts by affecting on heat distribution profile in a build job [10]. The motivation of this study is to provide new insights regarding the effects of process parameters on porosity formation in PBF-LB/M especially regarding the effect of scanning strategy there are few studies conducted with 316L. These scanning strategies govern the local heat distribution. When these effects are understood, switching to different patterns within a single build can simultaneously raise part quality and accelerate the process[3].

2. Material and equipment

Gas-atomised austenitic stainless-steel powder (316L) produced by SLM Solutions was employed. All samples were built on an Aconity MIDI+ (Aconity3D GmbH). The machine is equipped with a fibre laser and a controlled build chamber that allows adjustment of oxygen content below 100 ppm. Recommended baseline parameters for 316L supplied by Aconity GmbH served as the reference point for the present work. Scanning speed of 900 mm/s and hatch spacing of 0.08 mm and spot size of 0.08 mm is used for all specimens. Other specimen specific parameters are presented in Table1.

Table 1. Process parameters used in the study.

Sample ID	**1**	**2**	**3**	**4**	**5**	**6**	**7**	**8**	**9**
Scanning strategy	Simple	Simple	Simple	Stripe	Stripe	Stripe	Quad Islands	Quad Islands	Quad Islands
Laser power (W)	100	150	200	100	150	200	100	150	200

Scanning-strategy toolpaths were generated in Autodesk Netfabb® (Figure 1) and uploaded to the machine without further modification.

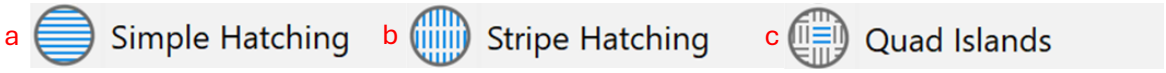

Figure 1. Representative scan-strategy patterns: (a) simple hatching, (b) stripe hatching, (c) quad-islands.)

3. Experimental procedure

Ten-millimetre cubes (10 × 10 × 10 mm^3) with a sacrificial support were oriented upright and distributed randomly across the build plate to minimise location bias. All nine parameter sets were produced in a single build.

For each specimen three non-overlapping fields of view were captured with an optical microscope and analysed in ImageJ. Greyscale thresholding separated pores (black) from bulk (white) to obtain an area-based porosity percentage. Images containing cracks were excluded because crack formation lay outside the study scope. Average porosity was plotted against laser power, specimen position and volumetric energy density according to equation 1 for comparison with literature. It is worth noting that sample with 100W laser power and simple hatching failed during the process and thus its place on the build plate is empty. Also, the neighbouring samples i.e. samples with 100W laser power and stripe hatching and 150W and quad islands hatching suffered from the uneven powder spreading.

4. Results and discussion

Figure 2 shows microscopy images revealing that pore morphology is strongly influenced by laser power. At laser power value of 100 W, pores are typically large and irregular, indicating lack-of-fusion defects. As laser power increases to 200 W, the pores become smaller and more spherical, suggesting more complete melting.

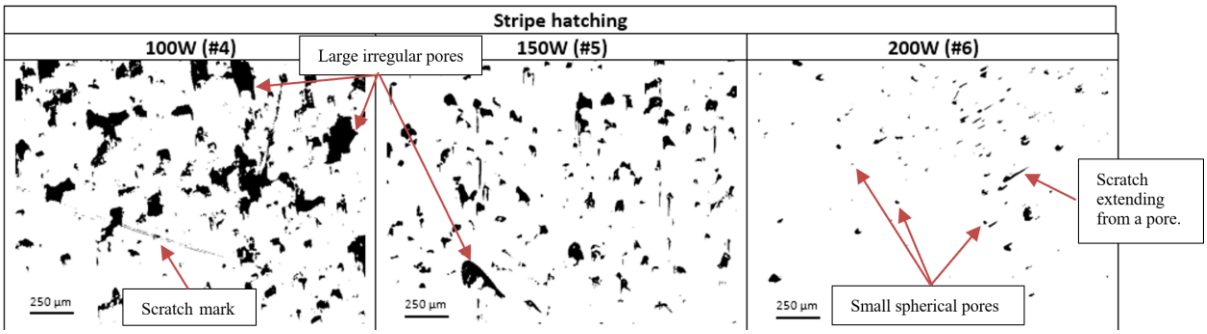

Figure 2. Pore size in different laser power (some elongated pore appearances were caused by surface scratches from insufficient polishing)

Figure 3a shows that, regardless of scan strategy, porosity steadily falls as laser power rises, reaching its minimum at 200 W. At low power (100 W), porosity peaks—especially in the first layers—because inadequate heat and poor plate bonding hinder fusion. By 150 W and 200 W, the energy is ample to melt consistently, so scan path has little effect and produces stable melt pools. However, at 100 W, stripe hatching outperforms quad island: continuous stripes overlap tracks more uniformly, whereas split islands heat unevenly, leaving unfused gaps. At higher powers, small differences reemerge—likely from keyholing or local powder-bed variations that trap gas or cluster pores in sensitive melt pools.

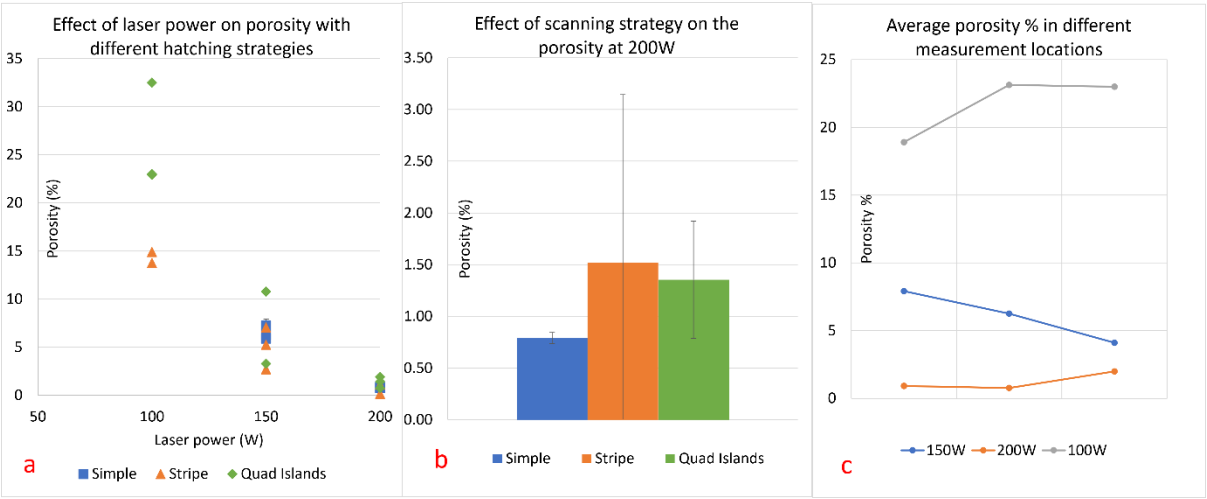

Figure 3a, b,c. a. a)Porosity as a function of laser power when different scanning strategies were used. b) Average porosities of samples manufactured with laser power of 200W. c) Average porosity in relation to the measuring location.

Figure 3b's error bars confirm that simple hatching yields the lowest porosity. Its uninterrupted heat flow and fewer start/stop points allow gases to escape before solidification. By contrast, stripe and island patterns introduce thermal interrupts that nucleate pores.

Finally, Figure 3c examines build height. At 150 W, porosity tapers toward the base, suggesting heat buildup over successive layers. But at both 100 W and 200 W, porosity slightly rises at the bottom: at 100 W, early-layer fusion is weakest; at 200 W, initial thermal losses destabilize the nascent melt pool.

Figure 4 shows a correlation between porosity and sample distortion. Higher porosity generally resulted in larger distortion, likely because internal voids reduce heat conduction and mechanical integrity. Localized heat accumulation and weakened structure due to porosity amplify warping effects during cooling.

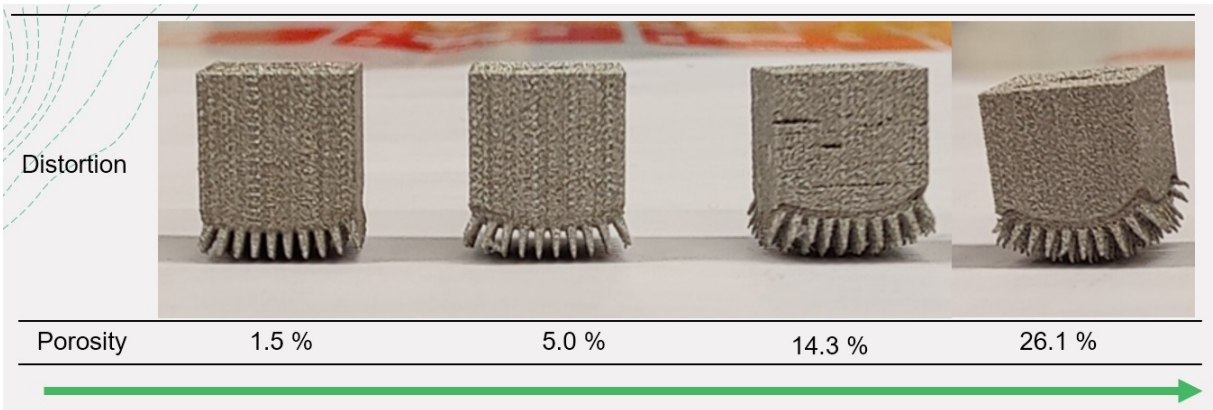

Figure 4. Correlation between porosity percentage and the distortion.

On the other hand, when laser powers of 100 W and 200 W were used, a subtle increase in porosity toward the bottom of the samples was observed. At the laser power of 100 W, the energy input may have been insufficient during the initial layers, leading to lack-of-fusion porosity. According to parameters recommended by manufacturer and Que et. al [14], laser power of 150W combined with simple hatching would result in minimal porosity. according to the results, when laser power value of 200W laser power was used the porosity were minimized. When the simple hatching strategy was applied with a laser power of 200 W, the lowest average porosity among the tested conditions was observed. However, notable variability within individual samples under this condition suggests that the result may not be statistically reliable. Therefore, no definitive conclusion can be drawn regarding the consistent superiority of the simple hatching strategy over the others. In the case of the stripe hatching, significant variation in porosity levels indicates that the PBF-LB/M process was unstable under these conditions. This instability may have originated from a failed build of one sample during the process, which visibly affected the surrounding samples.

The laser power of 200 W can be compared to values reported in the literature by converting it to volumetric energy density (*VED*), which results in a value of 93 J/mm^3. According to Lee [8] a critical *VED* of 79 J/mm^3 is required to achieve 99.5% density in 316L stainless steel. Furthermore, their results show that porosity continues to decrease as *VED* increases up to value of 155 J/mm^3. The porosity trend observed in this work follows a similar pattern when plotted as a function of *VED* and compared with the curve presented by Lee [8] though a consistent offset can be seen (Figure 5).

The offset may be due to differences in various parameters, like the used powder bed fusion machine, laser beam shape, size, and distribution. Additionally, Lee [8] reported that average pore size decreased as the *VED* increased, and similar phenomena was noticed in this study. This phenomenon can be explained by underlying melt pool dynamics. However, the conclusion by Lee [8] showed that porosity continues to decrease up to a *VED* of 155 J/mm^3—contrasts with the findings of Cherry et al. [1] who reported that the minimum porosity for 316L stainless steel was achieved at a *VED* of 105 J/mm^3. This discrepancy may be explained by differences in

processing regimes: beyond a certain energy density threshold, the mode of the PBF-LB/M process transitions from conduction mode to keyhole mode. Keyhole mode leads to deep, narrow melt pools that increase instability and gas pore entrapment, raising porosity.

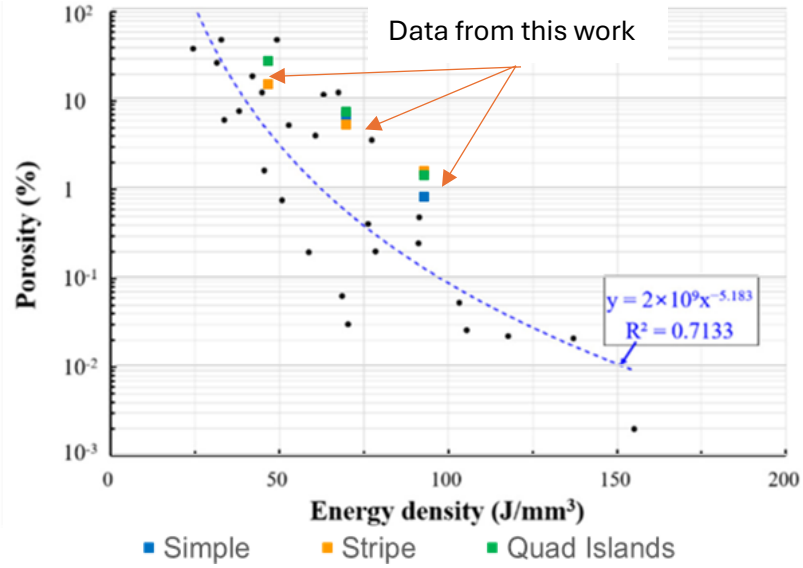

Figure 5. Porosity as a function of *VED*, by Lee H. [8]

5. Conclusions

This study investigated the influence of laser power and scanning strategy on porosity formation in 316L stainless steel components fabricated by PBF-LB/M. The results confirm that laser power plays a dominant role in determining porosity content, while the effect of scanning strategy remains less conclusive under the current experimental conditions. The lowest average porosity was achieved at a laser power of 200 W, corresponding to a volumetric energy density (*VED*) of 93 J/mm^3. This value aligns well with previous findings in the literature. This study did not explore higher energy densities, and observed deviations may be due to differences in equipment, beam characteristics, or scan parameters. Scanning strategy showed some influence at lower laser powers, with simple hatching yielding lower porosity than quad island hatching at 100 W. However, when high values of laser power (150 W and 200 W) were used, differences between strategies diminished, likely due to the overriding impact of energy input and potential build disturbances affecting local thermal conditions. Furthermore, porosity distribution within samples showed spatial dependence, particularly at laser power of 150W, where porosity decreased toward the bottom of the part. In contrast, samples with laser power of 200W showed slightly increased porosity at the lower regions, possibly due to early-stage thermal losses or insufficient heat accumulation at the start of the build. This study identifies a favourable energy density window for minimizing porosity in 316L stainless steel using PBF-LB/M, but highlights that further research, especially with more extensive data on scanning strategy and higher *VED* levels, is required to fully characterise and optimize the process.

Acknowledgements

The authors gratefully acknowledge the support of the Department of Mechanical and Materials Engineering at the University of Turku for providing the facilities and resources necessary to carry out this research.

References

1. Cherry, J. A., Davies, H. M., Mehmood, S., Lavery, N. P., Brown, S. G. R. and Sienz, J. 2015. Investigation into the effect of process parameters on microstructural and physical properties of 316L stainless steel parts by selective laser melting. *The International Journal of Advanced Manufacturing Technology*. **76**: 869–879.
2. Ghorbanpour, S., Deshmukh, K., Sahu, S., Riemslag, T., Reinton, E., Borisov, E., Popovich, A., Bertolo, V., Jiang, Q., Sanchez, M. T., Knezevic, M. and Popovich, V. 2022. Additive manufacturing of functionally graded inconel 718: Effect of heat treatment and building orientation on microstructure and fatigue behaviour. *J Mater Process Technol*. **306**: 117573.
3. Huang, X., Tian, X., Zhong, Q., He, S., Huo, C., Cao, Y., Tong, Z. and Li, D. 2024. High-Efficiency Dynamic Scanning Strategy for Powder Bed Fusion by Controlling Temperature Field of the Heat-Affected Zone. *Chinese Journal of Mechanical Engineering*. **37**: 22.
4. Jafari, D., van Alphen, K. J. H., Geurts, B. J., Wits, W. W., Gonzalez, L. C., Vaneker, T. H. J., Rahman, N. U., Römer, G. W. and Gibson, I. 2020. Porous materials additively manufactured at low energy: Single-layer manufacturing and characterization. *Mater Des*. **191**: 108654.
5. Jatti, V. S., Saiyathibrahim, A., Murali Krishnan, R., Jatti, A. V., Suganya Priyadharshini, G. and G. Mohan, D. 2025. Investigating the Effect of Volumetric Energy Density on Tensile Characteristics of As-Built and Heat-Treated AlSi10Mg Alloy Fabricated by Laser Powder Bed Fusion. *Adv Eng Mater*. **27**:.
6. Kantzos, C., Pauza, J., Cunningham, R., Narra, S. P., Beuth, J. and Rollett, A. 2019. An Investigation of Process Parameter Modifications on Additively Manufactured Inconel 718 Parts. *J Mater Eng Perform*. **28**: 620–626.
7. Kumar, P., Chakravarthy, P., Manwatkar, S. K. and Murty, S. V. S. N. 2021. Effect of Scan Speed and Laser Power on the Nature of Defects, Microstructures and Microhardness of 3D-Printed Inconel 718 Alloy. *J Mater Eng Perform*. **30**: 7057–7070.
8. Lee, H.-J. 2022. Effects of the Energy Density on Pores, Hardness, Surface Roughness, and Tensile Characteristics of Deposited ASTM 316L Specimens with Powder-Bed Fusion Process. *Materials*. **15**: 6672.
9. de Leon Nope, G. V., Perez-Andrade, L. I., Corona-Castuera, J., Espinosa-Arbelaez, D. G., Muñoz-Saldaña, J. and Alvarado-Orozco, J. M. 2021. Study of volumetric energy density limitations on the IN718 mesostructure and microstructure in laser powder bed fusion process. *J Manuf Process*. **64**: 1261–1272.
10. Liu, L., Wang, D., Yang, Y., Wang, Z., Qian, Z., Wu, S., Tang, J., Han, C. and Tan, C. 2023. Effect of Scanning Strategies on the Microstructure and Mechanical Properties of Inconel 718 Alloy Fabricated by Laser Powder Bed Fusion. *Adv Eng Mater*. **25**:.
11. Morano, C. and Pagnotta, L. 2024. On Powder Bed Fusion Manufactured Parts: Porosity and its Measurement. *Current Materials Science*. **17**: 185–197.
12. Newell, D. J., O'Hara, R. P., Cobb, G. R., Palazotto, A. N., Kirka, M. M., Burggraf, L. W. and Hess, J. A. 2019. Mitigation of scan strategy effects and material anisotropy through supersolvus annealing in LPBF IN718. *Materials Science and Engineering: A*. **764**: 138230.
13. Pfaff, A., Jäcklein, M., Schlager, M., Harwick, W., Hoschke, K. and Balle, F. 2020. An Empirical Approach for the Development of Process Parameters for Laser Powder Bed Fusion. *Materials*. **13**: 5400.
14. Qiu, C., Wang, Z., Aladawi, A. S., Kindi, M. Al, Hatmi, I. Al, Chen, H. and Chen, L. 2019. Influence of Laser Processing Strategy and Remelting on Surface Structure and Porosity Development during Selective Laser Melting of a Metallic Material. *Metallurgical and Materials Transactions A*. **50**: 4423–4434.
15. Ramirez, B., Banuelos, C., De La Cruz, A., Nabil, S. T., Arrieta, E., Murr, L. E., Wicker, R. B. and Medina, F. 2024. Effects of Process Parameters and Process Defects on the Flexural Fatigue Life of Ti-6Al-4V Fabricated by Laser Powder Bed Fusion. *Materials*. **17**: 4548.
16. Salem, H., Carter, L. N., Attallah, M. M. and Salem, H. G. 2019. Influence of processing parameters on internal porosity and types of defects formed in Ti6Al4V lattice structure fabricated by selective laser melting. *Materials Science and Engineering: A*. **767**: 138387.